

Comparisons of Carrington-Class Solar Particle Event Radiation Exposure Estimates on Mars utilizing the CAM, CAF, MAX, and FAX Human Body Models

A.M. Adamczyk,* C.M. Werneth, and L.W. Townsend

The University of Tennessee, Department of Nuclear Engineering
315 Pasqua Engineering Building, Knoxville, Tennessee, 37996-2300, United States of America

*adamczy@utk.edu

Estimating space radiation health risks for astronauts on the surface of Mars requires computational models for the space radiation environment, particle transport, and human body. In this work, estimates of radiation exposures as a function of altitude are made for a solar particle event proton radiation environment comparable to the Carrington event of 1859. The proton energy distribution for this Carrington-type event is assumed to be similar to that of the Band function fit of the February 1956 event. In this work, NASA's On-Line Tool for the Assessment of Radiation in Space (OLTARIS) was utilized for radiation exposure assessments. OLTARIS uses the deterministic radiation transport code HZETRN (High charge (Z) and Energy TRaNsport) 2010, which was originally developed at NASA Langley Research Center, to calculate the transport of charged particles and their nuclear reaction products through shielding materials and tissue. Exposure estimates for aluminum shield areal densities, similar to those provided by a spacesuit, surface lander, and permanent habitat, are calculated at the mean surface elevation and at an altitude of 8 km in the Mars atmosphere. Four human body models are utilized, namely the Computerized Anatomical Man (CAM), Computerized Anatomical Female (CAF), Male Adult voXel (MAX), and Female Adult voXel (FAX) models. Comparisons between the CAM and MAX model organ exposures, and similarly for CAF and FAX, are made since there are differences in the mass and location of various organs for the human body models. In addition, comparisons of the predicted organ exposures are made with current NASA Permissible Exposure Limits (PELs).

Keywords: *Space Radiation, Solar Particle Events, Extreme Space Weather, Dosimetry, Mars Exploration*

I. INTRODUCTION

Future space endeavors may include human exploration and habitation of Mars. During a human Mars mission, astronauts will be exposed to the harmful ionizing space radiation environment for extended periods of time. This hazardous environment consists of the omnipresent Galactic Cosmic Ray (GCR) background, and isolated Solar Particle Events (SPEs). Large SPEs are rare, but could pose significant health risks to crewmembers if adequate radiation shielding is not provided.

To provide a reasonable upper bound on the radiation doses during a SPE for a Mars surface mission, a realistic, hypothetical worst case SPE spectrum must be determined. Recent analyses [1, 2] on hypothetical worst case SPE spectra utilized an estimated SPE fluence based on the concentration of nitrates found in ice core samples spanning approximately the last 500 years [3]. During this 500 year period, the 1859 "Carrington" flare was the largest recorded SPE, thereby making it a favorable choice as a plausible worst case SPE. The Carrington event had the largest estimated omni-directional integral fluence of protons greater than 30 MeV (18.8×10^9 protons cm^2). To generate plausible spectra from this single fluence datum, previous studies [1, 2] assumed that the spectra shape was that of a large space age SPE (namely, the February 1956, November 1960, August 1972, or September 1989 event) re-normalized to the greater than 30 MeV Carrington proton fluence. It was

found that the radiation exposures using the generated plausible spectra were sensitive to the assumed spectral hardness. The hardest spectrum of the February 1956 event was shown to provide the largest, potentially lethal radiation dose [2]. Therefore, in this work the February 1956 energy spectrum normalized to the greater than 30 MeV Carrington proton fluence level was used for hypothetical worst case SPE radiation analyses.

This paper provides a description of the methodology required for SPE space radiation assessments during proposed Mars surface scenarios. The scenarios considered herein assume male and female astronauts located in a permanent habitat, surface lander, and spacesuit. Exposure related quantities relevant for comparisons to NASA permissible exposure limits (PELs) were calculated using NASA's On-Line Tool for the Assessment of Radiation in Space (OLTARIS) [4]. The mathematical models of the ambient space radiation environment, particle transport, and human body, required for this computational tool, are described herein.

To estimate space radiation health risks and ensure that space operations during each specific mission scenario meet NASA guidelines, organ dose and effective dose were calculated in four commonly used human phantoms. Comparisons between the Computerized Anatomical Man (CAM), Computerized Anatomical Female (CAF), Male Adult voXel (MAX), and Female Adult voXel (FAX) models are presented and analyzed since the differences in the mass and location of various organs in the human phantoms will affect these radiation exposure quantities.

II. COMPUTATIONAL METHODS

NASA's OLTARIS [4] was used to assess the effects of space radiation on male or female astronauts in a spacesuit, surface lander, and permanent habitat. This World Wide Web based tool calculates the transport of particles in the external environment through the shielding material and the astronaut's body. OLTARIS consists of three modules: environment definition, particle transport, and response functions. More details regarding these modules can be found in the subsequent sections.

A. Environment

The external radiation environment is defined in the environment module of OLTARIS. Users can select from six different types of environments, namely free space Galactic Cosmic Ray (GCR), free space SPE, lunar surface SPE, Earth orbit, or Jupiter's icy moon Europa. For this analysis, the free space SPE environment was used. When selecting this option, the user can then choose from a variety of historical SPEs or input a user defined proton spectrum utilizing four common proton spectral fitting methodologies, namely the Band function, an exponential in energy or rigidity, and Weibull fit.

The Band function parameterization [5, 6] of the February 1956 event was selected for the analysis presented herein, since it should yield more reliable dose estimates than other commonly used parameterizations, such as a Weibull fit. The Band function utilizes low and medium energy satellite data, as well as high energy (out to ~10 GeV) data obtained from ground level enhancements (GLEs) measured by neutron monitors on Earth's surface. As compared to the Weibull fit, which uses only low energy GLE data and extrapolates the proton energy spectra out to ~1 GeV, the Band function describes the entire proton energy spectrum. The Band function parameterization is given by

$$\Phi(>R) = \begin{cases} J_0 R^{-\gamma_1} \exp\left(-\frac{R}{R_0}\right), & \text{for } R \leq (\gamma_2 - \gamma_1)R_0 \\ J_0 R^{-\gamma_2} [(\gamma_2 - \gamma_1)R_0]^{(\gamma_2 - \gamma_1)} \exp(\gamma_1 - \gamma_2), & \text{for } R \geq (\gamma_2 - \gamma_1)R_0 \end{cases} \quad (1)$$

where Φ is the proton fluence, R is the particle rigidity (momentum per unit charge), J_0 is the total integral fluence, R_0 is the characteristic rigidity, and γ_1 and γ_2 are spectral indices. The spectral parameters J_0 , R , R_0 , γ_1 , and γ_2 for the Band function parameterization of the February 1956 SPE re-normalized to the September 1859 Carrington Event (used as input to OLTARIS) are given by 1.72×10^{10} protons cm^{-2} , 0.321 GV (gigavolts), 0.584, and 5.04, respectively. Using these spectral parameters,

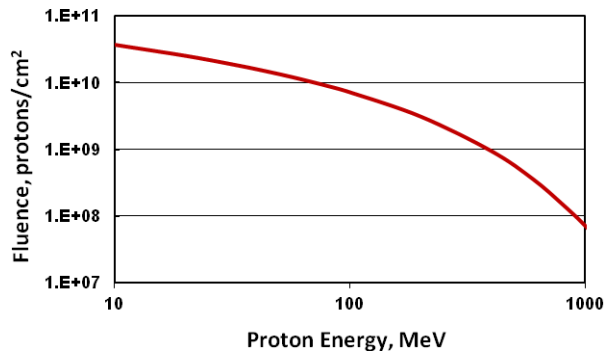


FIG. 1. Proton fluence spectrum for the Band function parameterization of the February 1956 event normalized to Carrington event of 1859.

the SPE proton fluence spectrum has been plotted and is displayed in Figure 1.

B. Particle Transport

The transport module of OLTARIS uses the deterministic space radiation transport code HZETRN (High charge (Z) and Energy TRAnsport) [7], which was developed at NASA Langley Research Center. HZETRN has been used extensively for both GCR and SPE dosimetric calculations using complex geometries. The transport algorithms of HZETRN provide approximate solutions to the time independent linear Boltzmann transport equation and utilize the straight ahead approximation and Continuous Slowing Down Approximation [8]. The code accurately models the transport of charged ions and their nuclear reaction products (protons, neutrons, deuterons, tritons, helions, and alpha particles).

Within the transport module, OLTARIS users can select from two transport scenarios, dependent on the type of geometry, namely a slab or thickness distribution. For this analysis, thickness distributions were created for the transport of the incident SPE proton spectrum through the Mars atmosphere (up to 300 g cm^{-2} CO_2), a hemispherical aluminum shielding thickness (0.3, 5, or 40 g cm^{-2}), and then tissue. As in previous Mars surface studies [2, 9, 10], the astronaut is assumed to be located on the surface of Mars in the center of three different aluminum hemispherical structures, each corresponding to the specific mission architectural element; an areal density of 0.3 g cm^{-2} represents a spacesuit, 5 g cm^{-2} characterizes a surface lander, and 40 g cm^{-2} indicates a permanent habitat. It should be noted that the ground level center location was selected since it is the location inside the hemisphere with the highest radiation exposures. For the Mars atmosphere, a spherically symmetric model of pure CO_2 composition was assumed with three areal densities namely low density (16 g cm^{-2}), high density (22 g cm^{-2}), and a density (7 g cm^{-2}) corresponding to an altitude of 8 km above the mean sur-

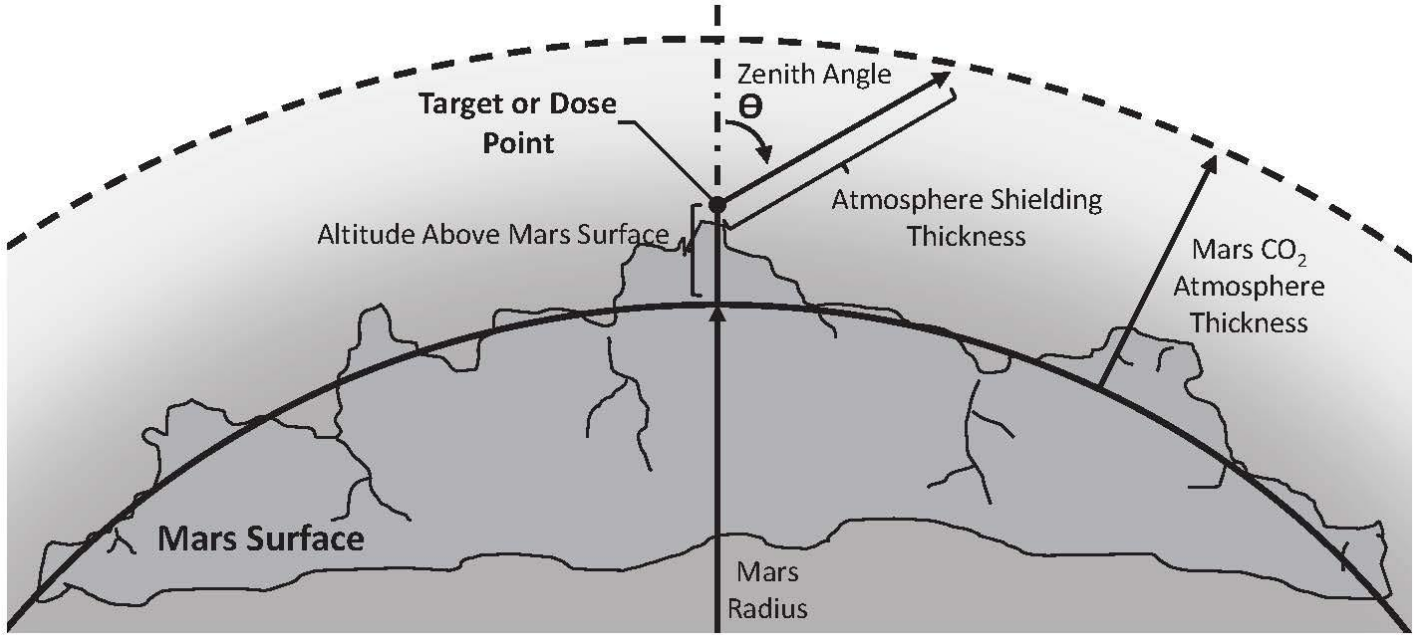


FIG. 2. Illustration of the Martian atmosphere geometry and description of the parameters associated with space radiation exposure calculations at a target point. Adapted from reference [12].

face elevation during low density atmosphere conditions [11-13].

The atmosphere shielding thicknesses (otherwise known as path lengths) are longer for particles arriving at angles greater than zero, with respect to the local zenith, due to the isotropic nature of SPE radiation. More information regarding the Mars atmosphere shielding thickness calculation can be found in references [12] and [13]. The Martian atmosphere geometry is illustrated in Figure 2. To account for the varying atmosphere shielding thicknesses, ray-tracing is required. The volume surrounding the target or dose point shown in Figure 2 is divided into a number of equal solid angle elements. The thickness of each type of shielding along a ray is then calculated through each solid angle element. Finally, a series of transport runs are computed of the external environment through the material thicknesses along the ray.

C. Radiation Exposure Calculations

The radiation exposure calculations presented herein were performed using OLTARIS. The response function module in OLTARIS allows users to compute dose, dose equivalent, linear energy transfer (LET), and/or whole body effective dose. This module calculates the response function, corresponding to each ray in the thickness distribution, by interpolating over a response function versus depth database. The total quantity at the target point of interest is calculated by integrating over all of the rays. The radiation exposure calculations presented herein are for the exposure on the Martian surface. Therefore, in this analysis the calculated directional response

is integrated over only the rays distributed in the 0 to 2π solid angle. The Martian surface provides planetary shielding over half of the solid angle. Therefore, the directional response in this case is assumed to be zero.

In this work, effective dose and organ dose are calculated for the three aluminum shield configurations as a function of elevation. For the effective dose calculations, OLTARIS combines the Mars atmosphere and aluminum shielding thickness distributions with the body thickness distributions for numerous organ or tissue target points in a human phantom. This process is repeated for each body target point and then a weighted average of these values is applied. OLTARIS calculates the effective dose using

$$E = \sum_T w_T H_T \quad (2)$$

where w_T is the tissue weighting factor for the organ or tissue denoted by T . OLTARIS uses the tissue weighting factors recommended in NCRP (National Council on Radiation Protection and Measurements) Report No. 132 [14]. The effective dose, given in equation (2), is calculated as a weighted average of the organ dose equivalent, H_T , which is expressed in units of centiSievert (cSv). Note that $1 \text{ cSv} = 0.01 \text{ Sv} = 1 \text{ rem}$ and $100 \text{ cSv} = 1 \text{ Sv} = 1 \text{ J kg}^{-1}$. The organ dose equivalent obtained from OLTARIS is calculated by the product of the ICRP (International Commission on Radiological Protection) Publication 60 [15] quality factor, Q , and organ dose, D . The organ dose is given in units of centiGray (cGy), where $1 \text{ cGy} = 0.01 \text{ Gy} = 1 \text{ rad}$ and $100 \text{ cGy} = 1 \text{ Gy} = 1 \text{ J kg}^{-1}$.

1. Human Body Models

OLTARIS users can select from four human body models. In the analysis presented herein, the CAM, CAF, MAX, and FAX human body models were utilized. It is recognized that additional human body models could have been used for this study; however, OLTARIS users are currently limited to the aforementioned phantoms.

The CAM and CAF human body models were developed in 1973 and 1992, respectively, to model the 50th percentile US Air Force male and female [16-18]. These mathematical geometric models are constructed using individual quadric surfaces that intersect to form closed three dimensional solids, which represent tissue and organs in the body [19].

The voxel-based body models, MAX and FAX, were developed in 2003 and 2004, respectively, by Kramer et al. [20, 21]. Voxels are used to specify data values within a regularly spaced, three dimensional grid. Arrays of cubic voxels compose the MAX and FAX models, where each voxel is associated with a specific tissue type [19]. Based on Computed Tomography (CT) scans of adult cadavers, the MAX and FAX body models were developed specifically to match the anatomical properties of the ICRP reference male and female [22].

The differences between the two sets of human body models, namely CAM/CAF and MAX/FAX, are anatomically based. A study conducted by Slaba et al. [19] found that differences in the mass and location of various organs impact organ dose equivalent calculations. Slaba et al. [19] concluded that for space radiation analyses, the voxel based MAX and FAX models provide a more accurate representation of the human body than the geometry based CAM and CAF models. Historically, the CAM and CAF models have been used extensively for NASA space radiation analyses, and more specifically, in many radiation exposure assessments for Martian surface missions [2, 9, 10]. Due to these reasons, the analyses presented herein will include both sets of human body models.

III. RESULTS

Martian surface organ doses and effective doses are estimated in this section for male and female astronauts located in a spacesuit, surface lander, and permanent habitat using the CAM, CAF, MAX, and FAX human body models. On the surface, the Mars atmosphere attenuates charged particle fluxes and provides a significant amount of radiation protection [13]. Therefore, it is expected that the Mars atmosphere will lower the organ and effective dose values and may offer enough additional atmospheric shielding to skew the differences between the two types of human body models.

A spherically symmetric CO₂ model was assumed for the Mars atmosphere with three areal densities, namely low density (16 g cm⁻²), areal densities, namely low density (16 g cm⁻²), high density (22 g cm⁻²), and a density (7 g cm⁻²) corresponding to an altitude of 8 km above the mean surface elevation during low density atmosphere conditions. At 8 km above the Martian surface, the organ and effective doses are expected to be larger due to the decreased SPE radiation attenuation.

It is recognized that the analyses presented herein ignore the radiation exposure incurred by astronauts enroute. A previous study examining Martian mission exposure determined that the highest radiation exposures are likely to occur during the Martian transit spaceflight [23]. Exposures on the Martian surface are expected to be lower due to the shielding provided by the Martian atmosphere and planet's bulk [9, 10]. However, significant radiation exposures will be incurred by astronauts on long duration Martian surface missions.

In this section, estimates of likely SPE organ doses are presented, due to their importance in assessments of short term health risks during specific Mars surface mission scenarios. In addition, effective dose values for SPE exposure incurred during individual mission segments are calculated since this exposure quantity is essential for space radiation cancer risk projections.

TABLE I. NASA PELs for short term or career non-cancer effects [24]. Note that N/A means not applicable.

Organ	30 day Limit (cGy-Eq)	1 Year Limit (cGy-Eq)	Career Limit (cGy-Eq)
Lens ^a	100	200	400
Skin	150	300	400
BFO	25	50	N/A
Heart ^b	25	50	100
CNS ^c	50	100	150
CNS ^c (Z ≥ 10)	—	10	25

^a Lens limits are intended to prevent early (<5 year) severe cataracts (for example, from a SPE).

^b Heart doses calculated as average over heart muscle and adjacent arteries.

^c CNS limits should be calculated at the hippocampus.

A. Organ Exposures

Keeping space radiation exposure within NASA permissible limits is necessary for Mars mission success and astronaut safety. Table I lists the PELs for non-cancer effects as defined in NASA Standard 3001, NASA Space Flight Human System Standard, Volume 1: Crew Health [24]. The thirty day, one year, and career limits are defined in units of centi-Gray-Equivalent (cGy-Eq) for the lens, skin, blood forming organs (BFO), heart, and central nervous system (CNS). Due to the high dose rate of a SPE, short term effects are of major concern. Therefore, during a SPE, it is important to keep radiation exposures below the thirty day NASA

TABLE II. Calculated skin doses, in units of cGy-Eq, for male and female astronauts on Mars surface utilizing the CAM, CAF, MAX, and FAX human body models. Results are given for high (22 g cm⁻²) and low density (16 g cm⁻²) atmospheres at the mean altitude (0 km) and at an altitude of 8 km for the low density atmosphere for the February 1956 SPE normalized to the Carrington event of September 1859. Skin doses in bold type exceed the 30 day PELs. Note that all doses are rounded to the nearest integer value.

Skin Dose (cGy-Eq)									
Human Body Models	0.3 g cm ⁻² Al Shield			5 g cm ⁻² Al Shield			40 g cm ⁻² Al Shield		
	Elevation (km) & Atmosphere Density			Elevation (km) & Atmosphere Density			Elevation (km) & Atmosphere Density		
	0 km	0 km	8 km	0 km	0 km	8 km	0 km	0 km	8 km
	High	Low	Low	High	Low	Low	High	Low	Low
CAM	118	161	268	102	137	214	50	62	81
CAF	119	162	270	103	138	215	51	62	82
MAX	122	169	285	105	142	224	51	63	83
FAX	123	169	286	106	143	225	51	63	84

TABLE III. Calculated lens doses, in units of cGy-Eq, for male and female astronauts on Mars surface utilizing the CAM, CAF, MAX, and FAX human body models. Results are given for high (22 g cm⁻²) and low density (16 g cm⁻²) atmospheres at the mean altitude (0 km) and at an altitude of 8 km for the low density atmosphere for the February 1956 SPE normalized to the Carrington event of September 1859. Lens doses in bold type exceed the 30 day PELs. Note that all doses are rounded to the nearest integer value.

Lens Dose (cGy-Eq)									
Human Body Models	0.3 g cm ⁻² Al Shield			5 g cm ⁻² Al Shield			40 g cm ⁻² Al Shield		
	Elevation (km) & Atmosphere Density			Elevation (km) & Atmosphere Density			Elevation (km) & Atmosphere Density		
	0 km	0 km	8 km	0 km	0 km	8 km	0 km	0 km	8 km
	High	Low	Low	High	Low	Low	High	Low	Low
CAM	116	158	251	102	135	206	52	63	82
CAF	117	158	254	103	137	209	52	64	83
MAX	114	154	246	100	132	201	51	62	81
FAX	116	157	251	101	135	205	51	63	82

PELs. Short term radiation exposures can lead to performance degradation, acute radiation syndrome (radiation sickness), or even death [24].

To compare the organ dose values calculated with OLTARIS to the NASA PELs, a multiplicative factor must be applied so that the organ dose values are expressed in units of cGy-Eq, as in Table I. In this work, the organ doses, D , calculated with OLTARIS, given units of cGy, were multiplied by a RBE (Relative Biological Effectiveness) value which accounts for the ability of some types of radiations to produce more short term and non-cancer damage than others for the same dose. To be more specific,

$$D[\text{cGy} - \text{Eq}] = D[\text{cGy}] \times \text{RBE} \quad (3)$$

where brackets are used to denote the units. Since SPEs primarily consist of protons, an RBE value of 1.5 was assumed, as recommended by NCRP Report 132 [14]. In this work, the calculated skin, lens, BFO, CNS, and heart doses are presented in Tables II-VI to allow for comparisons to the NASA PELs, given in Table I. To assess the short term effects of SPE radiation exposure, the organ doses given in Tables II-VI are compared to the thirty day NASA PELs. Analyses reveal that for the 0.3 g cm⁻² aluminum shielding configuration (which is comparable

to a spacesuit) with a low density atmosphere, all organ dose limits are exceeded for both genders at the mean altitude and at an altitude of 8 km. In addition, all male and female organ dose limits are exceeded for the 5 g cm⁻² aluminum shielding configuration (which is representative of a surface lander) with a low density atmosphere at an altitude of 8 km. In the subsequent paragraphs the specific organ doses will be compared to the NASA PELs.

Skin doses, shown in Table II, exceed the male and female NASA PELs for the two least shielded configurations, namely the 0.3 g cm⁻² aluminum shield with a low density atmosphere (16 g cm⁻²) at the mean altitude and at an altitude of 8 km. In addition, both genders exceed skin dose limits for the 5 g cm⁻² aluminum shielding configuration with a low density atmosphere at an altitude of 8 km. The short term effects due to exceeding the NASA skin PELs can include erythema, moist desquamation, and epilation [14, 25].

The lens doses, given in Table III, exceed the male and female limits for every atmosphere density and altitude combination of the spacesuit (0.3 g cm⁻² aluminum shield) and surface lander (5 g cm⁻² aluminum shield), with one exception; the lens dose limit is not exceeded for the MAX human body model in the surface lander with a high density atmosphere at the mean elevation. It

TABLE IV. Calculated BFO doses, in units of cGy-Eq, for male and female astronauts on Mars surface utilizing the CAM, CAF, MAX, and FAX human body models. Results are given for high (22 g cm^{-2}) and low density (16 g cm^{-2}) atmospheres at the mean altitude (0 km) and at an altitude of 8 km for the low density atmosphere for the February 1956 SPE normalized to the Carrington event of September 1859. BFO doses in bold type exceed the 30 day PELs. Note that all doses are rounded to the nearest integer value.

BFO Dose (cGy-Eq)									
Human Body Models	0.3 g cm ⁻² Al Shield			5 g cm ⁻² Al Shield			40 g cm ⁻² Al Shield		
	Elevation (km) & Atmosphere Density			Elevation (km) & Atmosphere Density			Elevation (km) & Atmosphere Density		
	0 km	0 km	8 km	0 km	0 km	8 km	0 km	0 km	8 km
	High	Low	Low	High	Low	Low	High	Low	Low
CAM	94	123	184	84	108	157	45	54	71
CAF	96	126	188	86	111	160	46	55	72
MAX	88	114	167	79	101	145	43	52	67
FAX	92	120	178	83	106	153	44	53	69

TABLE V. Calculated CNS doses, in units of cGy-Eq, for male and female astronauts on Mars surface utilizing the CAM, CAF, MAX, and FAX human body models. Results are given for high (22 g cm^{-2}) and low density (16 g cm^{-2}) atmospheres at the mean altitude (0 km) and at an altitude of 8 km for the low density atmosphere for the February 1956 SPE normalized to the Carrington event of September 1859. CNS doses in bold type exceed the 30 day PELs. Note that all doses are rounded to the nearest integer value.

CNS Dose (cGy-Eq)									
Human Body Models	0.3 g cm ⁻² Al Shield			5 g cm ⁻² Al Shield			40 g cm ⁻² Al Shield		
	Elevation (km) & Atmosphere Density			Elevation (km) & Atmosphere Density			Elevation (km) & Atmosphere Density		
	0 km	0 km	8 km	0 km	0 km	8 km	0 km	0 km	8 km
	High	Low	Low	High	Low	Low	High	Low	Low
CAM	101	133	199	91	117	170	48	58	75
CAF	103	137	206	93	121	176	49	59	76
MAX	100	130	194	89	115	166	47	57	73
FAX	101	133	200	91	118	171	48	58	75

TABLE VI. Calculated heart doses, in units of cGy-Eq, for male and female astronauts on Mars surface utilizing the CAM, CAF, MAX, and FAX human body models. Results are given for high (22 g cm^{-2}) and low density (16 g cm^{-2}) atmospheres at the mean altitude (0 km) and at an altitude of 8 km for the low density atmosphere for the February 1956 SPE normalized to the Carrington event of September 1859. Heart doses in bold type exceed the 30 day PELs. Note that all doses are rounded to the nearest integer value.

Heart Dose (cGy-Eq)									
Human Body Models	0.3 g cm ⁻² Al Shield			5 g cm ⁻² Al Shield			40 g cm ⁻² Al Shield		
	Elevation (km) & Atmosphere Density			Elevation (km) & Atmosphere Density			Elevation (km) & Atmosphere Density		
	0 km	0 km	8 km	0 km	0 km	8 km	0 km	0 km	8 km
	High	Low	Low	High	Low	Low	High	Low	Low
CAM	89	115	167	80	102	145	43	52	68
CAF	91	118	172	82	104	149	44	53	69
MAX	91	118	172	81	104	149	44	53	69
FAX	89	115	167	80	102	146	43	52	68

should be noted that none of the permanent habitat (40 cm⁻² aluminum shield), atmosphere, and altitude combinations exceed lens dose limits. Therefore, an acute radiation syndrome such as cataracts or keratitis [14] may occur in male and female astronauts unless they are located in the highest shielding configuration, which is the permanent habitat.

All of the BFO and heart doses shown in Tables IV and VI, respectively, exceed the NASA PELs. The space radiation doses delivered to these sensitive organ sites are likely to result in only hematological changes [14]. However, the radiation doses should be below the threshold for nausea and emesis.

The CNS doses, calculated with OLTARIS and given in Table V, exceed NASA PELs for mostly all of the aluminum shielding, atmosphere, and altitude combinations. Exceptions occur for all of the human body model CNS doses of the highest shielded combination, namely the 40 g cm⁻² aluminum shielding configuration with a high density atmosphere at the mean elevation. Exceeding the short term CNS radiation exposure PELs can lead to astronaut performance degradation due to behavioral changes or reductions in cognitive and motor function.

In addition to the comparisons between the specific organ doses and the NASA PELs, comparisons between

TABLE VII. Calculated effective doses, in units of cSv, for male and female astronauts on Mars surface utilizing the CAM, CAF, MAX, and FAX human body models. Results are given for high (22 g cm^{-2}) and low density (16 g cm^{-2}) atmospheres at the mean altitude (0 km) and at an altitude of 8 km for the low density atmosphere for the February 1956 SPE normalized to the Carrington event of September 1859. Note that all effective doses are rounded to the nearest integer value.

Effective Dose (cSv)									
Human Body Models	0.3 g cm ⁻² Al Shield			5 g cm ⁻² Al Shield			40 g cm ⁻² Al Shield		
	Elevation (km) & Atmosphere Density			Elevation (km) & Atmosphere Density			Elevation (km) & Atmosphere Density		
	0 km	0 km	8 km	0 km	0 km	8 km	0 km	0 km	8 km
	High	Low	Low	High	Low	Low	High	Low	Low
CAM	106	134	192	98	121	167	62	72	87
CAF	107	135	192	99	122	167	62	72	88
MAX	102	129	182	94	116	158	59	69	84
FAX	102	129	181	94	116	158	60	69	84

the CAM and MAX human body model organ doses, and similarly for CAF and FAX, are conducted. When comparing the skin doses of the two different types of human body models for each gender, it is found that MAX skin doses are larger than the CAM results. The FAX skin doses are larger than the CAF results, with one exception. Equal skin doses can be observed for the highest shielding combination, namely the 40 g cm^{-2} aluminum shielding configuration with a high density atmosphere at the mean altitude. The lens, BFO, and CNS doses give similar results for the two different types of human body models for each gender. For these three cases, the doses for the geometry based human body models, CAM and CAF, exceed the voxel based models, MAX and FAX. For the heart doses, different behavior is observed between the two different types of phantoms for males and females. The voxel based MAX model provides larger heart doses than the geometry based CAM model, although the geometry based CAF model results exceed the voxel based FAX model values.

In summary, a Carrington-type event with a spectrum similar to the February 1956 SPE, will likely result in organ exposures that exceed limits for any altitude in the Mars atmosphere and aluminum shielding configurations comparable to a spacesuit and surface lander. Organ limits may even be exceeded by male and female astronauts located in a permanent habitat. More specifically, the current thirty day NASA PELs for the BFO and heart, which are set at 25 cGy-Eq, are easily exceeded by male and female astronauts in all Mars mission architectural elements during a SPE. The conventional amount of shielding materials used in the construction of spacesuits, surface landers, and even permanent habitats will not provide the protection needed for the extreme event considered herein. To reduce radiation exposures to more acceptable levels during a SPE, a heavily shielded “storm shelter” could be added to a surface lander or permanent habitat. This possible shielding solution requires further investigation and may be included in future analyses.

B. Effective Dose

Table VII presents effective doses calculated with OLтарis for both male and female astronauts using the CAM, CAF, MAX, and FAX human body models. Results are displayed for high and low density atmospheres (as a function of altitude), in addition to the three aluminum shielding scenarios. The three shielding configurations are representative of a spacesuit (0.3 g cm^{-2}), surface lander (5 g cm^{-2}), and permanent habitat (40 g cm^{-2}), as mentioned previously.

TABLE VIII. NASA career PELs for astronauts on a one year mission [24].

Age (years)	Effective Dose (cSv)	
	Male	Female
25	52	37
30	62	47
35	72	55
40	80	62
45	95	75
50	115	92
55	147	112

Analyses of the effective dose results are complicated by the variety of comparisons that can be conducted. Comparisons of the effective dose results are made between the two different types of human body models for each gender (CAM versus MAX and CAF versus FAX), sets of phantoms (CAM/CAF versus MAX/FAX), and genders within the body model sets (CAM versus CAF and MAX versus FAX). A direct comparison between the two different types of human body models for each gender is made for Table VII. It can be seen that the geometry based CAM model has larger effective dose values than the voxel based MAX model for every possible shielding combination. Similarly, the geometry based CAF model results exceed the voxel based FAX results. Comparisons of the characteristically different sets of

TABLE IX. Age at first exposure (years) for which the effective dose values (given in Table VII) obtained using the CAM, CAF, MAX, and FAX human body models, exceed the NASA PELs of Table VIII. Results are given for high (22 g cm^{-2}) and low density (16 g cm^{-2}) atmospheres at the mean altitude (0 km) and at an altitude of 8 km for the low density atmosphere for the February 1956 SPE normalized to the Carrington event of September 1859. Note that the table entry “All” signifies that the NASA PELs are exceeded for all ages at first exposure.

Age ranges at first exposure (years) for which effective dose limits are exceeded.									
Human Body Models	0.3 g cm ⁻² Al Shield			5 g cm ⁻² Al Shield			40 g cm ⁻² Al Shield		
	Elevation (km) & Atmosphere Density			Elevation (km) & Atmosphere Density			Elevation (km) & Atmosphere Density		
	0 km High	0 km Low	8 km Low	0 km High	0 km Low	8 km Low	0 km High	0 km Low	8 km Low
CAM	25-45	25-50	All	25-45	25-50	All	25	25-30	25-40
CAF	25-50	All	All	25-50	All	All	25-35	25-40	25-45
MAX	25-45	25-50	All	25-40	25-50	All	25	25-30	25-40
FAX	25-50	All	All	25-50	All	All	25-35	25-40	25-45

human body models reveal that there is little difference between the calculated CAM/CAF and MAX/FAX effective doses for all shielding combinations with high and low density atmospheres at the mean altitude. The greatest difference between the CAM/CAF and MAX/FAX effective doses is seen for the least shielded configuration of the spacesuit and surface lander, namely the 0.3 g cm^{-2} and 5 g cm^{-2} aluminum shielding configurations with a low density atmosphere (16 g cm^{-2}) at an altitude of 8 km. Furthermore, comparisons of the genders within the sets of the human body are greater than or equal to those of CAM. Generally, the voxel based phantoms give similar results. FAX supplies effective doses which are greater than or equal to those of MAX, with one exception.

Table VIII lists the career effective dose limits, in units of cSv, for male and female astronauts on a one year mission. The limits are given as a function of age at first exposure, and established so as not to exceed a three percent risk of exposure induced death (REID) from carcinogenesis. For a NASA astronaut, this risk limit must not be exceeded at a 95 percent confidence level.

The relationship between space radiation exposure and carcinogenesis is age and gender specific. Note that all of the career effective dose limits listed in Table VIII increase with age due to latency effects of solid tumor formation. In addition, the limits are lower for female astronauts than male crewmembers at all ages. Gender differences in life span, as well as organ/tissue types and sensitivities, are factors in the risk projection calculations of these cumulative effective dose limits [24].

When comparing Tables VIII and VII it is readily apparent that that the effective dose limits are exceeded for a specific age at first exposure for every human body model, aluminum shielding configuration, atmosphere density, and elevation combination.

To simplify the comparisons, Table IX presents the age ranges at first exposure of male and female astronauts for which the effective doses, calculated with OLTARIS, exceed the NASA PELs. It can be seen in

Table IX, that both male human body models, namely CAM and MAX, and analogously for the female models CAF and FAX, give similar age ranges. More specifically, both male human body models (CAM and MAX) exceed effective dose limits for the same age ranges at first exposure with one exception for the 5 g cm^{-2} aluminum shield configuration with a high density atmosphere (22 g cm^{-2}) at the mean altitude. Both female human body models, namely CAF and FAX, give the same age ranges for the exceeded effective dose limits. Every human body model for all ages (at first exposure) exceed effective dose limits for the least shielded configuration of the spacesuit and surface lander. More explicitly, limits are exceeded for the 0.3 g cm^{-2} and 5 g cm^{-2} aluminum shielding configurations with a low density atmosphere (16 g cm^{-2}) at an altitude of 8 km.

In summary, only male and female astronauts older than 40 and 45 years, respectively, located in a permanent habitat (40 g cm^{-2} aluminum shield), will not exceed effective dose limits (for a one year mission) for all of the atmosphere density and altitude combinations considered herein. To reduce the potential radiation exposure during such an extreme event to tolerable levels, additional shielding scenarios will need to be investigated, such as locating the permanent habitat next to a vertical rise of a cliff or below the mean surface elevation in a narrow valley, canyon, crater, or cave.

IV. CONCLUSIONS

Radiation exposure estimates, from a SPE proton radiation environment comparable to the Carrington event of 1859, have been calculated for male and female astronauts on the surface of Mars and compared to NASA PELs. The computational tools and mathematical models incorporated into OLTARIS were used for the analyses presented herein. The SPE environment was defined as a Band function parameterization of the February 1956 incident proton spectrum, normalized to the greater than 30 MeV proton fluence of the Carrington event. OL-

TARIS utilizes the deterministic space radiation transport code HZETRN to calculate the transport of particles in the external environment through the shielding materials and human tissue. The incident SPE spectrum was transported through the Mars CO₂ atmosphere (for high and low density models at the mean elevation and at an elevation of 8 km) and three aluminum shielding configurations. These hemispherical aluminum configurations correspond to a spacesuit, surface lander, and permanent habitat. The CAM, CAF, MAX, and FAX human body models, which are readily available on OLTARIS, were used to represent the body self-shielding distributions for organs and tissues.

Organ doses and effective doses for male and female astronauts were calculated herein for various combinations of Mars atmosphere density, altitude, shielding configuration, and human body model. These results are an essential step to the determination of the space radiation shielding requirements during each architectural element of a Mars surface mission.

Comparisons of the organ dose and effective dose results were made between the two different types of human body models for each gender. Generally, for male astronauts the geometry based CAM model organ doses and effective doses exceed those of the voxel based MAX model. Similarly, for female astronauts the geometry based CAF model results generally were larger than the voxel based FAX results. It should be noted that overall, there are only small differences between the results of the two different types of human body models for each gender. Without the protection of the Mars CO₂ atmosphere, greater differences between the results of the human body models would be observed.

Furthermore, the calculated effective doses and organ doses were compared to NASA PELs. It was found that male and female astronauts older than 40 and 45 years, respectively, will not exceed effective dose limits for a one year mission when located in a permanent habitat for every atmosphere, altitude, and human body model combination. The resulting organ doses are generally found to exceed the NASA thirty day PELs. More specifically, the BFO and heart doses substantially exceed the NASA thirty day PELs. Exceeding the short term NASA PELs could lead to acute radiation syndrome responses, such as erythema, keratitis, or epilation, and astronaut performance degradation. These effects can potentially impact the completion of mission objectives, mission success, or possibly lead to death. To reduce the potential radiation exposure during a Carrington-type SPE to more acceptable levels, additional shielding scenarios will need to be investigated.

ACKNOWLEDGEMENTS

The authors would like to thank Dr. Tony Slaba for his helpful comments and many valuable discussions.

REFERENCES

- [1] L. Townsend, D. Stephens, J. Hoff, E. Zapp, H. Moussa, T. Miller, C. Campbell, and T. Nichols, *Advances in Space Research* **38**, 226 (2006).
- [2] L. Townsend, M. PourArsalan, M. Hall, J. Anderson, S. Bhatt, N. DeLauder, and A. Adamczyk, *Acta Astronautica* **69**, 397 (2011).
- [3] K. McCracken, G. Dreschhoff, D. Smart, and M. Shea, *Journal of Geophysical Research* **106**, 585 (2001).
- [4] R. Singleterry, S. Blattnig, M. Cloudsley, G. Qualls, C. Sandridge, L. Simonsen, T. Slaba, S. Walker, F. Badavi, J. Spangler, A. Aumann, E. Zapp, R. Rutledge, K. Lee, R. Norman, and J. Norbury, *Acta Astronautica* **68**, 1086 (2011).
- [5] D. Band, J. Matteson, L. Ford, B. Schaefer, D. Palmer, B. Teegarden, T. Cline, M. Briggs, W. Paciasas, G. Pendleton, G. Fishman, C. Kouveliotou, C. Meegan, R. Wilson, and P. Lestrade, *Astrophysical Journal* **413**, 281 (1993).
- [6] A. Tylka, W. Dietrich, and W. Atwell, in *Proceedings of the COSPAR XXXVIII Scientific Assembly, Paper F24-0004-10* (Bremen, Germany, 2010).
- [7] T. Slaba, S. Blattnig, and F. Badavi, *Journal of Computational Physics* **229**, 9397 (2010).
- [8] J. Wilson, L. Townsend, W. Schimmerling, G. Khandelwal, F. Khan, J. Nealy, F. Cucinotta, L. Simonsen, J. Shinn, and W. Norbury, *Transport Methods and Interactions for Space Radiations*, NASA Technical Report 1257 (1991).
- [9] L. Townsend, M. PourArsalan, and M. Hall, in *Proceedings of the 2010 IEEE Aerospace Conference* (Big Sky, Montana, 2010).
- [10] L. Townsend, M. PourArsalan, and M. Hall, in *Proceedings of the 40th International Conference on Environmental Systems (ICES), Paper No. AIAA 2010-6186* (Barcelona, Spain, 2010).

- [11] R. Smith and G. West, *Space and planetary environment criteria guidelines for use in space vehicle development, Volume 1: 1982 revision*, NASA Technical Memorandum 82478 (1983).
- [12] L. Simonsen, J. Nealy, L. Townsend, and J. Wilson, *Radiation Exposure for Manned Mars Surface Missions*, NASA Technical Paper 2979 (1990).
- [13] L. Simonsen and J. Nealy, *Mars Surface Radiation Exposure for Solar Maximum Conditions and 1989 Solar Proton Events*, NASA Technical Paper 3300 (1993).
- [14] National Council on Radiation Protection and Measurements (NCRP), "Radiation Protection Guidance for Activities in Low Earth Orbit," NCRP Report No. 132 (2000).
- [15] International Commission on Radiological Protection (ICRP), "The 1990 Recommendations of the International Commission on Radiological Protection," ICRP Publication 60 (1991).
- [16] M. Billings and W. Yucker, *The Computerized Anatomical Man (CAM) Model*, McDonnell Douglas Company (1973), Summary Final Report, MDC-G465.
- [17] W. Yucker and S. Huston, *The Computerized Anatomical Female*, McDonnell Douglas Company (1990), Final Report, MDC-6107.
- [18] W. Yucker and R. Reck, *The Computerized Anatomical Female Body Self-Shielding Distributions*, McDonnell Douglas Company (1992), Report, MDC 92H0749.
- [19] T. Slaba, G. Qualls, M. Cloudsley, S. Blattnig, S. Walker, and L. Simonsen, *Advances in Space Research* **45**, 866 (2010).
- [20] R. Kramer, J. Vieira, H. Khoury, F. Lima, and D. Fuelle, *Physics in Medicine and Biology* **48**, 1239 (2003).
- [21] R. Kramer, H. Khoury, J. Vieira, E. Loureiro, V. Lima, F. Lima, and G. Hoff, *Physics in Medicine and Biology* **49**, 5203 (2004).
- [22] International Commission on Radiological Protection (ICRP), "Basic Anatomical and Physiological Data for Use in Radiobiological Protection: Reference Values," ICRP Publication 89 (2001).
- [23] L. Townsend, F. Cucinotta, and J. Wilson, *Radiation Research* **129**, 48 (1992).
- [24] "NASA Space Flight Human System Standard – Volume 1: Crew Health," NASA-STD-3001 (2009).
- [25] National Council on Radiation Protection and Measurements (NCRP), "Guidance on radiation received in space activities," NCRP Report No. 98 (1989).